Short Communication

Altered spontaneous brain activity patterns in dysthyroid optic neuropathy: a resting-state fMRI study

Yi-Ping Jiang[1,†], Yan-Chang Yang[2,3,†], Li-Ying Tang[4], Qian-Min Ge[2], Wen-Qing Shi[2], Ting Su[2,5], Hui-Ye Shu[2], Yi-Cong Pan[2], Rong-Bin Liang[2], Qiu-Yu Li[2], Yi Shao[2,*]

[1] *Department of Ophthalmology, The First Affiliated Hospital of Gannan Medical University, 341000 Ganzhou, Jiangxi Province, China*

[2] *Department of Ophthalmology, The First Affiliated Hospital of Nanchang University, 330006 Nanchang, Jiangxi Province, China*

[3] *Department of Anesthesiology, First College for Clinical Medicine, Nanchang University, 330006 Nanchang, Jiangxi Province, China*

[4] *Department of Ophthalmology, Eye Institute of Xiamen University, School of Medicine, Xiamen University, Zhongshan Hospital, Xiamen University, 361102 Xiamen, Fujian Province, China*

[5] *Department of Ophthalmology, Massachusetts Eye and Ear, Harvard Medical School, Boston, MA 02114, USA*

*Correspondence: freebee99@163.com (Yi Shao)
[†]These authors contributed equally.

DOI:10.31083/j.jin2002037

Submitted: 12 March 2021 Revised: 2 April 2021 Accepted: 14 April 2021 Published: 30 June 2021

This research investigates the characteristics of spontaneous brain activity in dysthyroid optic neuropathy patients using the regional homogeneity technique. Sixteen patients with dysthyroid optic neuropathy and 16 thyroid-associated ophthalmopathy patients without dysthyroid optic neuropathy were recruited, matched for weight, height, age, sex, and educational level. All participants underwent resting-state functional nuclear resonance imaging, and the characteristics of spontaneous brain activity were evaluated using the regional homogeneity technique. Each participant in the dysthyroid optic neuropathy group also completed the Hospital Anxiety and Depression scale. Receiver operating characteristic curves were used to compare brain activity between the two groups. Pearson correlation analysis evaluated the relationship between regional homogeneity and clinical manifestations in dysthyroid optic neuropathy patients. In addition, we analyzed the correlation between Hospital Anxiety and Depression scale and regional homogeneity. We found that the regional homogeneity values at the corpus callosum/cingulate gyrus and parietal lobe/middle frontal gyrus significantly decreased in dysthyroid optic neuropathy patients. Regional homogeneity values at the corpus callosum/cingulate gyrus and parietal lobe/middle frontal gyrus were negatively correlated with Hospital Anxiety and Depression scale and disease duration. It was found that the regional homogeneity signal values were significantly lower than in thyroid-associated ophthalmopathy without in dysthyroid optic neuropathy, which may indicate a risk of regional brain dysfunction in dysthyroid optic neuropathy. The results show that regional homogeneity has the potential for early diagnosis and prevent dysthyroid optic neuropathy. In addition, the findings suggest possible mechanisms of dysthyroid optic neuropathy optic nerve injury. They may provide a valuable basis for further research on the pathological mechanisms of dysthyroid optic neuropathy.

Keywords

Dysthyroid optic neuropathy; Regional homogeneity; Thyroid-associated ophthalmopathy; Resting-state fMRI; Hospital Anxiety and Depression

1. Introduction

Thyroid-associated ophthalmopathy (TAO) is a common extrathyroid autoimmune disease involving orbital tissue. In severe cases, irreversible visual impairment can be caused by corneal ulcers and optic neuropathy [1]. Dysthyroid optic neuropathy (DON) is the most severe complication, with an incidence of 4%–8% [2] in TAO patients. The early symptoms of TAO are subtle and can gradually develop into vision loss, visual field defect, color vision abnormality, and even blindness [3].

The pathophysiological mechanism of DON may be as follows: (1) The most widely accepted view is that the related immune-mediated inflammatory response activates and releases a large number of inflammatory mediators, secreting hydrophilic glycosaminoglycans and causing extraocular muscle swelling which directly compresses the optic nerve at the orbital apex [4]; (2) Retinal ganglion cell (RGC) damage may be caused by high intraocular pressure [5]; (3) Excessive orbital content may cause stretching and injury of the optic nerve [6]; (4) Optic nerve fiber compression and obstructed circulation may result in denervated atrophy [7]. The visual pathway leads from RGC axons to the occipital lobe of the visual cortex. It is composed of the optic nerve, optic chiasm, optic tract and optic radiations. Lesions in different parts of the pathway can lead to different degrees of visual impairment [8].

Thyroid hormones play essential roles in neuron differentiation, neuron formation, myelination and synaptic production [9]. In rats, a decrease in serum thyroid hormone level has been found to decrease myelin basic protein expression and number of oligodendrocytes, leading to abnormal optic nerve function [10]. Thyroid disease patients commonly have visual dysfunction, with the abnormality of correspond-

Journal of Integrative Neuroscience

ing brain regions [11]. Thus, visual pathway anomalies in DON may be accompanied by visual dysfunction, and early detection is vital for timely diagnosis and treatment of DON.

Magnetic resonance imaging (MRI) is a standard technology in clinical diagnosis and biological research. It has gradually become the most widely used imaging method with an annual growth rate of 12% and has begun to replace invasive biopsy as a diagnostic method [12]. In addition, MRI has been widely used in the study of brain structure and function. Functional magnetic resonance imaging (fMRI) is based on the blood oxygen level-dependent (BOLD) effect, reflecting regional brain neural activity under different conditions, and achieving the goal of non-invasive specific observation of brain function *in vivo* [13]. The use of this approach to analyze the visual pathway and related brain regions may be helpful in the study of pathogenesis and pathophysiology of eye disease.

In an active brain region, the responses within voxels are consistent in time series. Regional homogeneity (ReHo) reflects the degree of synchronization of neuronal activities in the brain region by calculating the temporal consistency of each voxel with its adjacent voxels. An increase in ReHo value indicates the more homogeneous activity of functional neurons in the local brain region, while reduced ReHo points to more disordered activity. ReHo accurately and reliably reflects visual information processing and can study brain activity in eye disease. Our previous research has successfully used the ReHo method to evaluate the internal ulcer [14], diabetic retinopathy [15], late monocular blindness [16], classic trigeminal neuralgia [17], acute eye pain [18], retinal detachment [19], universal acute open-globe injury [20], diabetic vitreous pathogenesis [21], optical neuritis [22], comitant strabismus [23], and strabismus with amblyopia [24]. Therefore, ReHo is of great significance in evaluating spontaneous brain activity.

2. Materials and methods

2.1 Subjects

From October 2016 to October 2019, 16 DON patients and 16 TAO patients without DON were recruited (all patients were diagnosed by doctors with the title of attending doctor or above in the Ophthalmology and Endocrinology Department). Six males and ten females were included in each group, and the two groups were matched in age, height and education level. The hospital ethics committee approved the study and in accordance with the Helsinki declaration. After being informed about the trial and its potential risks, each participant signed a declaration of informed consent.

Selection criteria for all participants were as follows: (1) Age 20–70 years; (2) Meeting the classic TAO diagnostic criteria established by Bartley in 1995 (exophthalmos with protrusion $\geq$19 mm and interocular difference $>$2 mm, or extraocular muscle involvement with hypertrophy and limited eye movement), specifically thyroid dysfunction with eyelid retraction or without eyelid retraction but with abnormal exophthalmos, optic nerve dysfunction or extraocular muscle involvement. Patients with similar signs caused by other eye diseases were excluded; (3) No previous eye surgery, hormone, radiotherapy, or immunosuppressive treatment. The diagnostic criteria for DON patients, based on clinical records, were as follows: TAO patients with visual impairment and having at least one of the following criteria: (i) Best-corrected visual acuity $<$0.8; (ii) Visual mean defect (MD) $<$-5 dB; (iii) Significant abnormality in visual evoked potential (VEP); (iv) Abnormal pupil light reflex; (v) Color vision abnormality. Fundus lesions caused by DON can be seen in Fig. 1.

Participants with TAO and without DON had no symptoms indicative of DON.

Patients with the following conditions were excluded from either group: (1) Ocular symptoms or visual abnormalities caused by eye pain, retinal disease, cataract, glaucoma or other conditions; (2) Corneal ulcer caused by the incomplete eyelid closure characteristic of TAO; (3) Systemic disease including hypertension, heart disease, diabetes, cerebrovascular disease, or brain trauma; (4) Psychiatric or neurological disease; (5) Patients with drug addiction.

2.2 MRI parameters

DON patients were diagnosed as DON by ophthalmologists and endocrinologists and underwent MRI examination after hospitalization. A trio 3-Tesla MRI scanner (Siemens Healtineers) was used for MRI recording, with the participant in an awake, quiet state with eyes closed. The duration of the scanning sequence was 15 min and it included 176 structural images and 240 functional images. The specific parameters are shown in Table 1.

2.3 Functional magnetic resonance imaging data analysis

MRIcro software (www.mricro.com) was used to classify the data and to exclude incomplete data. To maintain the magnetization balance, the first 15 time points were discarded. Using the advanced version of rs-fMRI data processing assistant (DPARSFA 4.0, http://rfmri.org/DPARSF), head movement was corrected, and the spatial position and slice timing were normalizedthe form conversion of medical digital imaging communication (DICM) was completed. The full-width smoothing was performed using the rs-fMRI data analysis tool (REST) and statistical parameter mapping software (SPM8), using a Gaussian kernel function at six $\times$ six $\times$ six mm^3. Data with displacement of at least 1.5 mm along the x, y or z axis or angular displacement were excluded from the analysis. Head motion artifacts were removed using the six-motion parameter technique. The standard echo plane image template was used to ensure data met the spatial standard of the Montreal Neurological Institute (MNI). Images were detrended and bandpass-filtered (0.01–0.08 Hz) to improve accuracy and reduce bias caused by respiratory or cardiac noise.

2.4 Correlation analysis

All patients completed the Hospital Anxiety and Depression Scale (HADS). Graphpad prism 8 (GraphPad Software

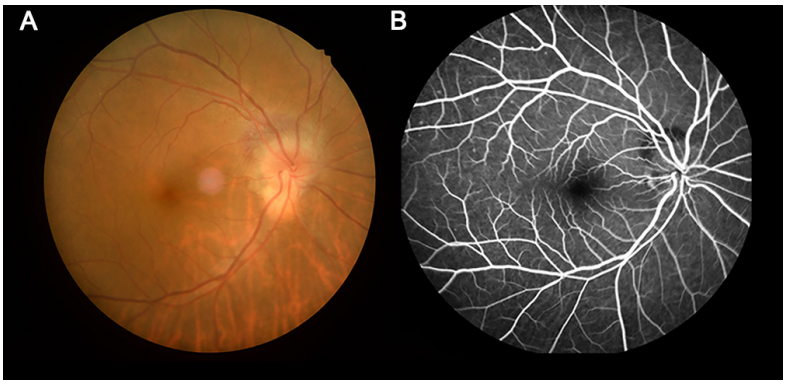

Fig. 1. Example of dysthyroid optic neuropathy seen on fundus camera and fluorescence fundus angiography. Fundus color images (A) showed optic papillomedema with ill-defined boundaries and no significant change in FFA (B).

Table 1. Information About MRI Parameters.

Data acquisition	Scanning parameters of structural images	Scanning parameters of functional images
Patient		
Sex		
Male	6	6
Female	10	10
Age, average range	54.85 ± 5.02	53.09 ± 5.16
Scan parameters		
Repetition time/echo time	1900/2.26 ms	2000/30 ms
Thickness/gap	1.0/0.5 mm	4.0/1.2 mm
Acquisition matrix	256 × 256	64 × 64
Field of view	250 × 250 mm	220 × 220 mm
Flip angle	90°	90°

Abbreviations: MRI, magnetic resonance imaging.

Inc., San Diego, CA, USA) was used to analyze the relationship between HADS and ReHo in the corpus callosum/cingulate gyrus and parietal lobe/middle frontal gyrus using a criterion P-value of < 0.001.

2.5 Statistical analysis

SPSS version 24.0 (SPSS Inc, Chicago, IL, USA) software was used to compare demographic and clinical data. P values less than 0.05 were considered statistically significant. Voxel activity was compared between the two groups using the REST software (http://www.restfmri.net). When performing multiple comparison corrections, the statistical threshold of voxel-level was 0.05. Receiver operating characteristic (ROC) curves were used to analyze changes in the ReHo values of DON patients. In addition, the Pearson correlation analysis method was used to explore the linear correlation between ReHo values and HADS in specific brain regions.

2.6 Ethical approval

All research methods were in accordance with the 1964 Helsinki declaration and its later amendments or comparable ethical standards.

3. Results

3.1 Demographics and visual measurements

No significant difference between the groups in terms of gender, age, weight or handedness. However, there were differences between the two groups in BCVA-right ($P < 0.05$) and BCVA-left ($P < 0.05$). See Table 2 for details.

3.2 ReHo differences

ReHo values at the corpus callosum/cingulate gyrus and the parietal lobe/middle frontal gyrus were significantly lower in the DON group than the TAO group (see Fig. 2 and Table 3 for details).

3.3 Correlation analysis

In the DON group, the ReHo values at the corpus callosum/cingulate gyrus and the parietal lobe/middle frontal gyrus were negatively correlated with HADS scores (r = –0.931 and –0.894 respectively; $P < 0.001$) and with duration of DON (r = –0.883 and –0.865 respectively; $P < 0.001$) (Fig. 3).

3.4 ROC curve

We speculated that the ReHo value could potentially be used as an index to distinguish the DON group from other TAO participants. To test this hypothesis, brain region-specific ReHo values of recordings from DON participants were plotted using ROC curves.

Table 2. Basic information of participants.

Condition	DON	TAO without DON	*t*	*P*-value*
Male/female	6/10	6/10	N/A	>0.99
Age (years)	54.85 ± 5.02	53.09 ± 5.16	0.218	0.714
Weight (kg)	64.12 ± 7.16	59.16 ± 7.06	0.125	0.902
Handedness	16R	16R	N/A	>0.99
Duration of DON (ws)	3.81 ± 1.94	N/A	N/A	N/A
Best-corrected VA-left eye	0.35 ± 0.20	1.05 ± 0.10	−3.137	0.012
Best-corrected VA-right eye	0.55 ± 0.25	1.05 ± 0.10	−3.783	0.021
Latency (ms)-right of the VEP	123.12 ± 10.04	103.04 ± 5.26	3.731	0.007
Amplitudes(uv)-right of the VEP	6.61 ± 2.32	14.19 ± 1.67	−7.542	0.004
Latency (ms)-left of the VEP	119.12 ± 8.32	101.12 ± 3.61	5.395	0.011
Amplitudes (uv)-left of the VEP	11.09 ± 3.17	15.12 ± 2.52	−4.135	0.011

Notes: Independent *t*-tests comparing two groups ($P < 0.05$).

Abbreviations: DON, dysthyroid optic neuropathy; TAO, thyroid-associated ophthalmopathy; HCs, healthy controls; N/A, not applicable; VA, visual acuity; VEP, visual evoked potential; R, right.

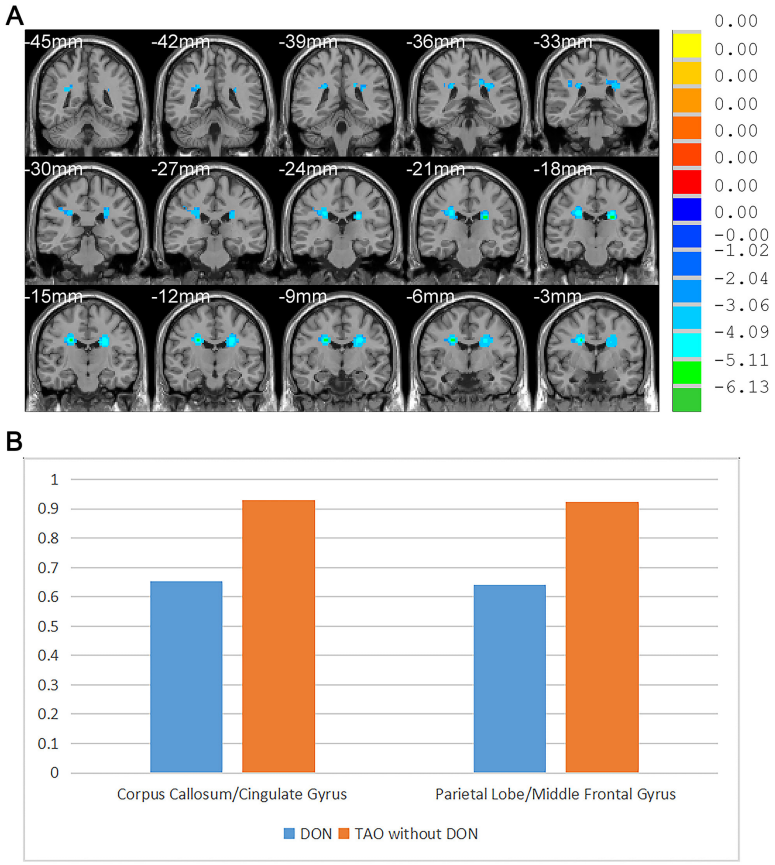

Fig. 2. Spontaneous brain activity in DON and TAO groups. (A) Blue shadow represents the strength of the signals. The corpus callosum/cingulate gyrus and parietal lobe/middle frontal gyrus exhibit lower signals ($P < 0.005$ for multiple comparisons using Gaussian random field theory, cluster >99 voxels, AlphaSim corrected). (B) The mean ReHo signal value between the two groups. ReHo values at the corpus callosum/cingulate gyrus and the parietal lobe/middle frontal gyrus were significantly lower in the DON group than in the TAO group.

Abbreviations: DON, dysthyroid optic neuropathy; TAO, thyroid-associated ophthalmopathy; ReHo, Regional Homogeneity.

As shown in Fig. 4, the areas under the ROC curves were 0.933 ($P < 0.0001$; 95% CI: 0.821–1.000) for the corpus callosum/cingulate gyrus and 0.938 ($P < 0.0001$; 95% CI: 0.826–1.000) for parietal lobe/middle frontal gyrus.

4. Discussion

The purpose was to investigate whether there are differences in the ReHo values of the brain regions of TAO patients with and without DON. The research results may provide a

Table 3. Brain areas with significantly different ReHo values between the DON and TAO without DON.

Brain areas	MNI coordinates			Number of voxels	*t* value
	X	Y	Z		
DON < TAO without DON					
Corpus callosum/cingulate gyrus	−21	−21	24	621	−5.3864
Parietal lobe/middle frontal gyrus	21	0	30	638	−5.3204

Notes: The statistical threshold was set at a voxel level with $P < 0.005$ for multiple comparisons using Gaussian random field theory (AlphaSim corrected at cluster >99 voxels, $P < 0.05$).

Abbreviations: ReHo, Regional Homogeneity; TAO, thyroid-associated ophthalmopathy; MNI, Montreal Neurological Institute; DON, dysthyroid optic neuropathy.

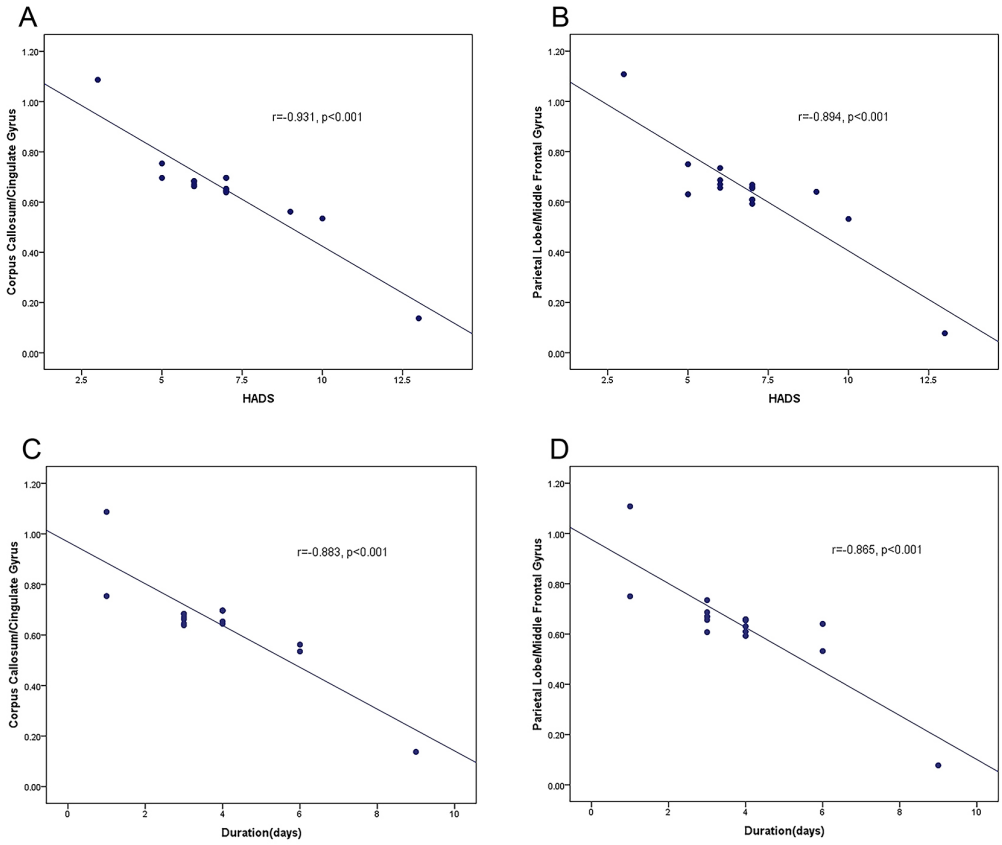

Fig. 3. The correlations of HADS scores and signal values in different brain regions. (A) The ReHo values at the corpus callosum/cingulate gyrus were negatively correlated with HADS scores. (B) The ReHo values at the parietal lobe/middle frontal gyrus were negatively correlated with HADS scores. (C) The ReHo values at the corpus callosum/cingulate gyrus were negatively correlated with duration of DON. (D) The ReHo values at the parietal lobe/middle frontal gyrus were negatively correlated with duration of DON.

Abbreviations: HADS, Hospital Anxiety and Depression Scale; ReHo, Regional Homogeneity; DON, dysthyroid optic neuropathy.

basis for the early diagnosis of DON in TAO patients, allowing timely intervention to halt or slow disease progression. The ReHo method was also used in our previous studies on anomalies in neural brain function (Table 4, Ref. [14–24]).

As shown in Fig. 5, the ReHo values at the corpus callosum/cingulate gyrus and parietal lobe/middle frontal gyrus were significantly decreased in DON patients. The corpus callosum is a bundle of fibers connecting the left and right cerebral hemispheres. Its pathological changes can cause intellectual disability, disturbance of consciousness, psychiatric and behavioral abnormalities [25]. The cingulate gyrus, located between the cingulate sulcus and the corpus callosum sulcus, is the cortical component of the limbic system [26]. However, the functions of the anterior and posterior cingulate gyri are not the same. The anterior cingulate gyrus is related to many complex physical and visceral motor functions and pain responses.

In contrast, the posterior cingulate gyrus is involved in monitoring of sensory, stereotactic, and memory functions [27]. In addition, the posterior cingulate gyrus plays a vital

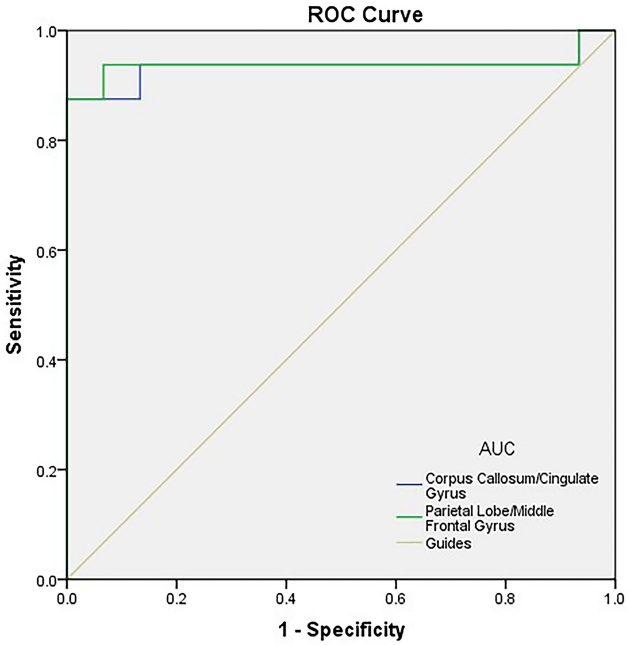

Fig. 4. ROC curve analysis of the mean ReHo values for altered brain regions. The area under the ROC curve were 0.933 ($P < 0.0001$; 95% CI: 0.821–1.000) for Corpus Callosum/Cingulate Gyrus, and 0.938 ($P < 0.0001$; 95% CI: 0.826–1.000) for the Parietal Lobe/Middle Frontal Gyrus.

role in eye movement and visuospatial processing [28]. The cingulate cortex is composed of different anatomical fields. Neuroimaging studies have shown that different cingulate cortex areas have mutual sensory, social, and goal-directed information processing activities [29]. Studies of mild cognitive impairment in Parkinson's disease have found that the thickness of the anterior cingulate cortex (ACC) and posterior cingulate cortex (PCC) is reduced, and regional cerebral blood flow changes in the PCC and anterior and middle cingulate cortex are associated with levels of language intelligence quotient and ACC executive function. In addition, the cingulate cortex is associated with apathy and visual hallucination [30], with the neural projection from ACC to ventral hippocampus controlling the expression of contextual fear generalization [31]. A functional connectivity analysis showed that traumatic exposure might lead to abnormal local and network connectivity in individuals with or without post-traumatic stress disorder, with reduced connectivity between the dorsal anterior cingulate cortex and the right hippocampus [32]. According to the "emotion theory", signals related to emotion travel via the hippocampus, fornix, papillary body and anterior thalamic nucleus to the cingulate gyrus known as the 'emotional cortex'. Stereotactic lesions of the bilateral anterior cingulate gyrus have been found to treat refractory mental disorders [33].

We observed that the ReHo values at the corpus callosum/cingulate gyrus were significantly reduced in DON, indicating that the neural activity in this area was decreased. We speculate that this is due to the abnormal visual pathway

Table 4. Regional Homogeneity method applied in ophthalmological diseases.

Author	Year	Disease
Xu MW *et al.* [14]	2019	corneal ulcer
Liao XL *et al.* [15]	2019	diabetic retinopathy
Huang X *et al.* [16]	2017	late monocular blindness
Xiang CQ *et al.* [17]	2019	classic trigeminal neuralgia
Tang LY *et al.* [18]	2018	acute eye pain
Huang X *et al.* [19]	2017	retinal detachment
Huang X *et al.* [20]	2016	universal acute open-globe injury
Zhang YQ *et al.* [21]	2020	diabetic vital pathogenesis
Shao Y *et al.* [22]	2015	optical neuritis
Huang X *et al.* [23]	2016	comitant strabismus
Shao Y *et al.* [24]	2019	strabismus and amblyopia

caused by optic neuropathy, consistent with the abnormal visual function found in DON patients. In addition, correlation analysis showed that weak corpus callosum/cingulate gyrus activity occurred in participants with higher levels of anxiety and depression and longer duration of DON, which may indicate that DON patients are more prone to anxiety and depression.

The parietal lobe is located behind the central sulcus. The transverse parietal sulcus divides the parietal lobe into superior and inferior parietal lobules. This lobe supports the advanced cognitive functions of human beings. Its size is related to mathematical and logical abilities; in particular, the size of the posterior parietal lobe is positively correlated with these functions [34]. Studies have shown that the parietal lobe plays a vital role in language processing. It integrates sensory and motor information, a function closely related to transforming voice-based expression into instructions to drive action [35]. The sensory information of the primary and secondary somatosensory areas reaches the lower parietal lobe through the upper parietal lobe. Visual sensory information is processed by the dorsal visual pathway and reaches the inferior parietal lobule, the inner parietal sulcus and the precuneus lobe.

In contrast, auditory information is transmitted from the posterior parietal lobe. The inferior parietal lobe and the inner parietal sulcus are related to upper limb movement and memory, suggesting somatic, audiovisual and vestibular sensory information processing, and even an essential role in cognition and movement [36]. It should be noted that the cortex of the posterior parietal lobe is the critical node in the anatomical network connecting the visual and (anterior) frontal cortex, temporal lobe and part of the frontal cortex. The upper longitudinal tract and its components work together with the arcuate and middle longitudinal tracts to transmit visual function [37]. Since the middle frontal gyrus mediates the interaction between dorsal and ventral attention networks (VANs) and is connected with the two networks, attentional control plays an essential role[38]. Transcranial stimulation of the middle frontal gyrus affects the critical nodes of the time-varying brain network, resulting

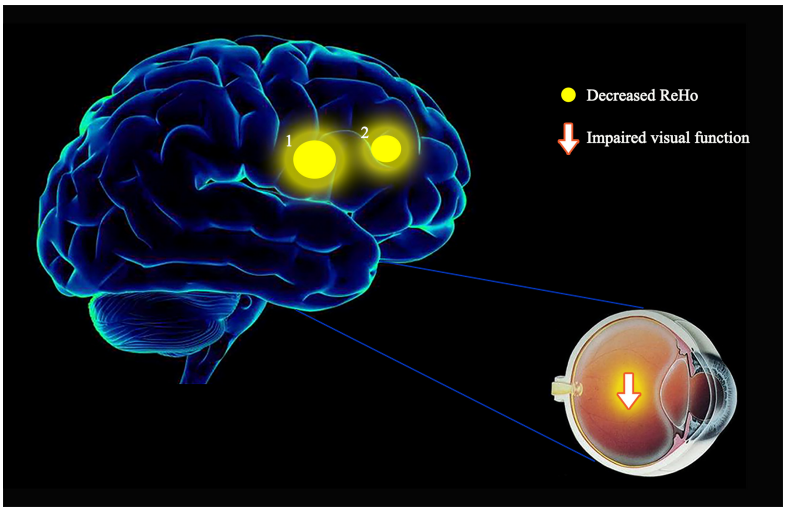

Fig. 5. The mean ReHo values of altered brain regions. Compared with the TAO, the ReHo values of the following regions were decreased to various extents: 1—Corpus Callosum/Cingulate Gyrus (t = −5.3864), 2—Parietal Lobe/Middle Frontal Gyrus (t = −5.3204).
Abbreviations: DON, dysthyroid optic neuropathy; TAO, thyroid-associated ophthalmopathy; ReHo, Regional Homogeneity.

Table 5. Brain region alternation and its potential impact.

Brain regions	Experimental result	Brain function	Anticipated results
Corpus callosum/Cingulate gyrus	DON < TAO without DON	Advanced neurological, physical, mental and visceral activity, pain response, sensory monitoring and stereotactic, and memory	Emotional and memory disorders, behavioral abnormalities, hallucinations, slow reaction and other mental disorders, hunger, thirst, sexual behavior abnormalities, gastrointestinal peristalsis and other visceral dysfunction symptoms
Left inferior temporal gyrus	DON < TAO without DON	High cognitive function, vision, language understanding and emotion regulation	Cognitive impairment, facial agnosia, semantic dementia and emotional disorder

Abbreviations: DON, dysthyroid optic neuropathy; TAO, thyroid-associated ophthalmopathy.

in the reorganization of the brain network module [39]. In addition, studies have shown that the middle frontal gyrus is associated with memory storage, executive and decision-making abilities and depression [40].

Reduced parietal lobe/middle frontal gyrus ReHo values in the DON group may indicate decreased neural activity in this region. The HADS score was negatively correlated with the ReHo value of parietal lobe/middle frontal gyrus (r = −0.894; $P < 0.001$), indicating that the decrease of ReHo score in DON is accompanied by an increased HADS score and suggesting that DON patients are more prone to anxiety and depression than TAO patients without DON. In addition, the duration of DON was negatively correlated with the ReHo value at the parietal lobe/middle frontal gyrus, suggesting a reduced function in this region with prolongation and progression of the disease. This may reflect changes to brain network nodes in this region, resulting in the impairment of related brain functions, and suggests a pathological mechanism of DON.

5. Conclusions

The ReHo method was used to investigate the changes in neural activity and brain function in DON patients. It was found that the ReHo signal values of the cortex callosum/cingulate gyrus and parietal lobe/middle frontal gyrus in DON were significantly lower than in TAO without DON, which may indicate a risk of regional brain dysfunction in DON (Table 5). Once DON occurs, it can cause severe symptoms such as eye pain, diplopia, blurred vision, and even blindness. The results demonstrate that ReHo has potential as a method of early diagnosis and prevention of DON. In addition, the findings suggest possible mechanisms of DON optic nerve injury, which have been poorly understood, and may provide a valuable basis for further work on the pathological mechanisms of DON. However, it is worth noting that there are still some limitations in our work, such as small sample size, may lead to biased results, samples from the same hospital may have regional bias, the MRI scanning process may have artifacts due to patient uncertainty, etc. In our future research, we will modify and improve the above aspects to make the research results more reliable.

Abbreviations

DON, dysthyroid optic neuropathy; ReHo, Regional Homogeneity; TAO, thyroid-associated ophthalmopathy; rs-fMRI, resting-state functional nuclear resonance imaging; HADS, Hospital Anxiety and Depression; ROC, Receiver operating characteristic; AUC, area under the curve.

Author contributions

YPJ and YS conceived and designed the experiments; LYT performed the experiments; YCY, QMG, WQS, TS and HYS analyzed the data; YCP, RBL and QYL contributed reagents and materials; YPJ and YCY wrote the paper.

Ethics approval and consent to participate

All research methods were approved by the medical ethics committee of the First Affiliated Hospital of Nanchang University and were in accordance with the 1964 Helsinki declaration and its later amendments or comparable ethical standards. All subjects have explained the purpose, method, potential risks and signed an informed consent form.

Acknowledgment

We thank anonymous reviewers for their excellent criticism of the article.

Funding

This research is supported by Central Government Guides Local Science and Technology Development Foundation (No: 20211ZDG02003); Key Research Foundation of Jiangxi Province (No: 20181BBG70004, 20203BBG73059); Excellent Talents Development Project of Jiangxi Province (No: 20192BCBL23020); Natural Science Foundation of Jiangxi Province (No: 20181BAB205034); Grassroots Health Appropriate Technology "Spark Promotion Plan" Project of Jiangxi Province (No: 20188003); Health Development Planning Commission Science Foundation of Jiangxi Province (No: 20201032, 202130210); Health Development Planning Commission Science TCM Foundation of Jiangxi Province (No: 2018A060, 2020A0087); Education Department Foundation of Jiangxi Province (No: GJJ200157, GJJ200159, GJJ200169).

Conflict of interest

The authors declare no conflict of interest.

Availability of data and materials

The data relating to this experiment can be obtained from the corresponding authors.

References

[1] Zhang Y, Li X, Guo C, Dong J, Liao L. Mechanisms of Spica Prunellae against thyroid-associated Ophthalmopathy based on network pharmacology and molecular docking. BMC Complementary Medicine and Therapies. 2020; 20: 229.

[2] Yu B. Predictive parameters on CT scan for dysthyroid optic neuropathy. International Journal of Ophthalmology. 2020; 13: 1266–1271.

[3] Bahn RS. Graves' ophthalmopathy. New England Journal of Medicine. 2010; 362: 726–738.

[4] Joseph SS, Miller NR. Management of dysthyroid optic neuropathy. In Mukherjee B., Yuen H. (eds.) Emergencies of the Orbit and Adnexa (pp. 235–257). New Delhi: Springer. 2017.

[5] Zah-Bi G, Abeillon-du Payrat J, Vie AL, Bournaud-Salinas C, Jouanneau E, Berhouma M. Minimal-access endoscopic endonasal management of dysthyroid optic neuropathy: the dysthone study. Neurosurgery. 2019; 85: E1059–E1067.

[6] Gonçalves ACP, Silva LN, Gebrim EMMS, Matayoshi S, Monteiro MLR. Predicting dysthyroid optic neuropathy using computed tomography volumetric analyses of orbital structures. Clinics. 2012; 67: 891–896.

[7] Gonçalves AC, Silva LN, Gebrim EM, Monteiro ML, Monteiro MLR. Quantification of orbital apex crowding for screening of dysthyroid optic neuropathy using multidetector CT. American Journal of Neuroradiology. 2012; 33: 1602–1607.

[8] Gupta M, Bordoni B. Neuroanatomy, visual pathway. Treasure Island: StatPearls Publishing. 2021.

[9] Demeneix B. Evidence for prenatal exposure to thyroid disruptors and adverse effects on brain development. European Thyroid Journal. 2019; 8: 283–292.

[10] Özkan B, Anik Y, Katre B, Altintaş Ö, Gençtürk M, Yüksel N. Quantitative assessment of optic nerve with diffusion tensor imaging in patients with thyroid orbitopathy. Ophthalmic Plastic and Reconstructive Surgery. 2015; 31: 391–395.

[11] Dai H, Morelli JN, Ai F, Yin D, Hu C, Xu D, *et al.* Resting-state functional MRI: functional connectivity analysis of the visual cortex in primary open-angle glaucoma patients. Human Brain Mapping. 2013; 34: 2455–2463.

[12] Bhuva AN, Moralee R, Moon JC, Manisty CH. Making MRI available for patients with cardiac implantable electronic devices: growing need and barriers to change. European Radiology. 2020; 30: 1378–1384.

[13] Yurgelun-Todd DA, Renshaw PF, Goldsmith P, Uz T, Macek TA. A randomized, placebo-controlled, phase 1 study to evaluate the effects of TAK-063 on ketamine-induced changes in fMRI BOLD signal in healthy subjects. Psychopharmacology. 2020; 237: 317–328.

[14] Xu M, Liu H, Tan G, Su T, Xiang C, Wu W, *et al.* Altered regional homogeneity in patients with corneal ulcer: a resting-state functional MRI study. Frontiers in Neuroscience. 2019; 13: 743.

[15] Liao X, Yuan Q, Shi W, Li B, Su T, Lin Q, *et al.* Altered brain activity in patients with diabetic retinopathy using regional homogeneity: a resting-state fMRI study. Endocrine Practice. 2019; 25: 320–327.

[16] Huang X, Ye C, Zhong Y, Ye L, Yang Q, Li H, *et al.* Altered regional homogeneity in patients with late monocular blindness: a resting-state functional MRI study. Neuroreport. 2017; 28: 1085–1091.

[17] Xiang C, Liu W, Xu Q, Su T, Yong-Qiang S, Min Y, *et al.* Altered spontaneous brain activity in patients with classical trigeminal neuralgia using regional homogeneity: a resting-state functional MRI study. Pain Practice. 2019; 19: 397–406.

[18] Tang L, Li H, Huang X, Bao J, Sethi Z, Ye L, *et al.* Assessment of synchronous neural activities revealed by regional homogeneity in individuals with acute eye pain: a resting-state functional magnetic resonance imaging study. Journal of Pain Research. 2018; 11: 843–850.

[19] Huang X, Li D, Li HJ, Zhong YL, Freeberg S, Bao J, *et al.* Abnormal regional spontaneous neural activity in visual pathway in retinal detachment patients: a resting-state functional MRI study. Neuropsychiatric Disease and Treatment. 2017; 13: 2849–2854.

[20] Huang X, Li HJ, Ye L, Zhang Y, Wei R, Zhong YL, *et al.* Altered regional homogeneity in patients with unilateral acute open-globe injury: a resting-state functional MRI study. Neuropsychiatric Disease and Treatment. 2016; 12: 1901–1906.

[21] Zhang Y, Zhu F, Tang L, Li B, Zhu P, Shi W, *et al.* Altered regional homogeneity in patients with diabetic vitreous hemorrhage. World Journal of Diabetes. 2020; 11: 501–513.

[22] Shao Y, Cai F, Zhong Y, Huang X, Zhang Y, Hu P, *et al.* Altered intrinsic regional spontaneous brain activity in patients with optic neuritis: a resting-state functional magnetic resonance imaging study. Neuropsychiatric Disease and Treatment. 2015; 11: 3065–3073.

[23] Huang X, Li S, Zhou F, Zhang Y, Zhong Y, Cai F, *et al.* Altered intrinsic regional brain spontaneous activity in patients with comitant strabismus: a resting-state functional MRI study. Neuropsychiatric Disease and Treatment. 2016; 12: 1303–1308.

[24] Shao Y, Li Q, Li B, Lin Q, Su T, Shi W, *et al.* Altered brain activity in patients with strabismus and amblyopia detected by analysis of regional homogeneity: a resting-state functional magnetic resonance imaging study. Molecular Medicine Reports. 2019; 19: 4832–4840.
[25] Bartley GB, Gorman CA. Diagnostic criteria for Graves' ophthalmopathy. American Journal of Ophthalmology. 1995; 119: 792–795.
[26] Satterthwaite TD, Elliott MA, Gerraty RT, Ruparel K, Loughead J, Calkins ME, *et al.* An improved framework for confound regression and filtering for control of motion artifact in the preprocessing of resting-state functional connectivity data. NeuroImage. 2013; 64: 240–256.
[27] Chaudhari D, Renjen PN, Arora AS. Acute corpus callosum infarct. Neurology India. 2019; 67: 930–931.
[28] Rolls ET. Limbic systems for emotion and for memory, but no single limbic system. Cortex. 2015; 62: 119–157.
[29] Rolls ET. The cingulate cortex and limbic systems for action, emotion, and memory. Cingulate Cortex. 2019; 166: 23–37.
[30] Yu YJ, Liang RB, Yang QC, Ge QM, Li QY, Li B, *et al.* Altered spontaneous brain activity patterns in patients after Lasik surgery using amplitude of low-frequency fluctuation: a resting-state functional MRI study. Neuropsychiatric Disease and Treatment. 2020; 16: 1907–1917.
[31] Kolling N, Behrens T, Wittmann MK, Rushworth M. Multiple signals in anterior cingulate cortex. Current Opinion in Neurobiology. 2016; 37: 36–43.
[32] Vogt BA. Cingulate cortex in Parkinson's disease. Cingulate Cortex. 2019; 60: 253–266.
[33] Bian X, Qin C, Cai C, Zhou Y, Tao Y, Lin Y, *et al.* Anterior cingulate cortex to ventral hippocampus circuit mediates contextual fear generalization. Journal of Neuroscience. 2019; 39: 5728–5739.
[34] Chen HJ, Zhang L, Ke J, Qi R, Xu Q, Zhong Y, *et al.* Altered resting-state dorsal anterior cingulate cortex functional connectivity in patients with post-traumatic stress disorder. Australian & New Zealand Journal of Psychiatry. 2019; 53: 68–79.
[35] Coslett HB, Schwartz MF. The parietal lobe and language. Handbook of Clinical Neurology. 2018; 151: 365–375.
[36] Kobayashi Y. Neuroanatomy of the parietal association areas. Brain and Nerve. 2016; 68: 1301–1312.
[37] Caspers S, Zilles K. Microarchitecture and connectivity of the parietal lobe. Handbook of Clinical Neurology. 2018; 151: 53–72.
[38] Wu Y, Wang J, Zhang Y, Zheng D, Zhang J, Rong M, *et al.* The neuroanatomical basis for posterior superior parietal lobule control lateralization of visuospatial attention. Frontiers in Neuroanatomy. 2016; 10: 32.
[39] Song P, Lin H, Liu C, Jiang Y, Lin Y, Xue Q, *et al.* Transcranial magnetic stimulation to the middle frontal gyrus during attention modes induced dynamic module reconfiguration in brain networks. Frontiers in Neuroinformatics. 2019; 13: 22.
[40] Wu YY, Yuan Q, Li B, Lin Q, Zhu PW, Min YL, *et al.* Altered spontaneous brain activity patterns in patients with retinal vein occlusion indicated by the amplitude of low-frequency fluctuation: a functional magnetic resonance imaging study. Experimental and Therapeutic Medicine. 2019; 18: 2063–2071.